An Optimal Triple-Series Parallel-Ladder Topology for Maximum Power Harvesting Under Partial Shading Conditions

Sarayu Vunnam*‡, M. Vanithasri**, RamakoteswaraRao Alla***

*Research Scholar, Department of Electrical Engineering, Annamalai University, Tamilnadu, India.

**Associate Professor, Department of Electrical Engineering, Annamalai University, Tamilnadu, India.

***Associate Professor, Department of EEE, RVR & JC College of Engineering, Andhra Pradesh, India.

(sarayu.vunnam@gmail.com, vanithasimman@yahoo.com, ramnitkkr@gmail.com)

‡Corresponding Author; V.Sarayu, Assistant Professor, Department of EEE, RVR & JC College of Engineering, Guntur, Andhra Pradesh, India-522019. Tel: +91 9989509419, sarayu.vunnam@gmail.com

Received: 31.01.2023 Accepted:13.04.2023

Abstract- Over the past few years, renewable energy has significantly contributed to the field of energy markets. Many photovoltaic (PV) array installations demonstrate the growing importance of solar energy. However, when operating under partial shading conditions (PSC), photovoltaic plants exhibit variable irradiance, which leads to low output power. Selection of the proper PV material and configuration are essential in overcoming this issue. This paper proposes a novel Triple-Series Parallel-Ladder Topology (T-SP-L) with monocrystalline PV material to maximize the output power under PSC. To comment on the effectiveness of the proposed topology, a 6x6 size PV array has been considered and compared with other topologies such as Series-Parallel (S-P), Honey-Comb (H-C), Total-Cross-Tied (T-C-T), Bridge-Link (B-L) considering Long Narrow (LN), Short Narrow (SN), Short Wide (SW), Long Wide (LW) and Middle (M) shading situations.

Keywords PV Material; Mono crystalline; Photo Voltaic Array; Total-Cross-Tied; Triple- Series Parallel-Ladder Topology.

1. Introduction

The world is currently experiencing an energy catastrophe as a result of the non-renewable energy sources beginning to deplete at an increasing rate. Consequently, using more renewable sources of energy, like solar, wind, tidal, etc., is the most obvious solution to solve this problem. Power semiconductor technology has undergone significant development over time [1]. Solar energy is now one of the most sought-after alternatives because the cost of photovoltaic cells has significantly decreased. In addition, sunlight has the extra benefit of being accessible and not polluting the environment. Although solar energy is extensively available, its extraction is constrained by some limitations. Because of some factors, including variations in solar radiation, the impact of shadowing, and an increase in solar cell hotness, the performance of PV systems is negatively impacted [2]. Due to nearby structures, trees, street light poles, and other factors, photovoltaic plants deployed in urban areas frequently operate under partial shade conditions. As a result, PV plants produce less output power, may experience hot-spot issues and may have a shorter lifespan overall.

To handle heavy load demands, the interconnection of PV modules is essential since a single PV module gives less power and is less efficient. The modules may be linked in parallel or in series. The series connections results in greater voltage at output, which is the sum of the voltages of distinct arrays. The current in series connection is restricted to each module current [3]. Although the power produced in this case is unquestionably more excellent than that of an individual module, it can only support intermediate power loads. The same is true for parallel connections, where the system voltage is constrained to the voltage of each module, and addition of all individual modules current gives system current [4]. Therefore, various interconnection schemes, including series-parallel, honeycomb, total cross tied and bridge linked, are recommended for solar PV systems to handle high power loads. TCT design outperforms others because of extracting maximum power. The solar PV array experiences an uneven distribution of shadow due to partial shading. As a result, partial shade significantly affects PV and IV characteristics and the array's decreased power yield.

PV characteristics also effected due to partial shading results in multiple peak points. Authors in [12] analyzed various 5X5 PV array configurations performance with different shading patterns. Effects of illumination and temperature for enhancing the effectiveness of photovoltaic systems has been addressed in [19]. It is reported that TCT configuration results are superior to others. A PV configuration with triple tied connection has been suggested by authors in [13], the suggested configuration results are validated by considering 7x7 size PV array. The photovoltaic temperature challenges are investigated in [14].

The type of PV material, cell temperature, cloud and other shading things, etc., influence the PV system efficiency. The intrinsic characteristic of the semiconductor material also plays a major role in influencing efficiency [6]. The quantity of energy conversion also depends on material used for the panel since the amount of light reaching the solar cell depends on the material quality; hence the material selection is critical in producing PV cells [8]. The most commonly used panel materials are Thin-film, Polycrystalline and Monocrystalline type. The most popular solar panels are thin-film ones made of cadmium telluride (CdTe) [5]. The CdTe layer may be sandwiched within two translucent conducting layers to help the thin-film screen engross light. A similar kind of thin-film technology frequently has a protective glass covering applied. By using amorphous silicon (a-Si) material also solar panels category of thin film can be manufactured [7]. Even though they do include silicon, solid silicon wafers are not used to make these thin film panels. Instead, they cover glass, plastic, or metal with non-crystalline silicon. Performance analysis of 6x6 T-C-T PV arrays based on Thin Film, Poly Crystalline and Mono Crystalline materials under several partial shading situations has been examined by [9] and resolved that the Mono Crystalline material based PV system outperforms than thin-film and poly crystalline material based PV system. A.D. Dhass researched the performance evaluation of various PV materials, including germanium, cadmium telluride, silicon, gallium arsenide and indium phosphide in [10].

Performance enhancement of PV Systems using fuzzy logic has been reported in [29]. The application of machine learning algorithms for maximum power improvement has been done by authors in [30-31]. The amount of power harvested from the total array is negatively impacted by the position of shaded in the PV array. PV reconfiguration, a crucial method for overcoming this important restriction, involves physically or electrically switching the location of the PV modules. As a result of this inspiration, the authors in [32] suggest a novel PV reconfiguration method based on an enhanced heterogeneous hunger games search optimizer (EHHGS). A thorough analysis of cutting-edge technologies with a range of control strategies, focusing on the relative benefits and effects on power grids are reported in [33]. An enhanced three-level Neutral Point Clamped (NPC) inverter connects a Solar PV system with Maximum Power Point Tracking (MPPT) with a battery storage system in a grid-integrated system has been developed in [34].

Novel contributions of the paper are:

- This paper proposes a novel Monocrystalline photovoltaic material-based 6X6 Triple-Series Parallel-Ladder Topology (T-SP-L).
- Performance analysis of proposed configuration has been done under PSCs.
- Comparative analysis with existing configurations has been done.
- The importance of Monocrystalline material based PV configuration has been highlighted.

The remaining part of the manuscript is organized as: the importance of monocrystalline based PV panels and various existing PV array configurations along with proposed configuration are described in section 2. The shading conditions used to analyze the performance of PV configurations are discussed in section 3. Section 4 gives the performance analysis with discussions. The conclusions drawn are listed in section 5.

2. Monocrystalline Material Based PV Array Configurations

Importance of monocrystalline material and various PV array configurations based on monocrystalline PV material are described in this section. Monocrystalline solar cells are the market's most extensively used and active solar cells. Single crystalline cells are another name for monocrystalline solar cells [11]. Due to their deep black colour and curved edges, they are easily recognized. Monocrystalline solar cells are the most effective when converting sunlight into electricity because they are manufactured from a complete form of silicon [15]. Additionally, monocrystalline-based solar cells take up much less space than other types. They indeed require the least amount of space than other solar cell technologies [16]. They are the solar cell technology with the highest durability advantage, with a life expectancy now anticipated to be over fifty years [17]. Fig. 1 shows the Monocrystalline PV module structure

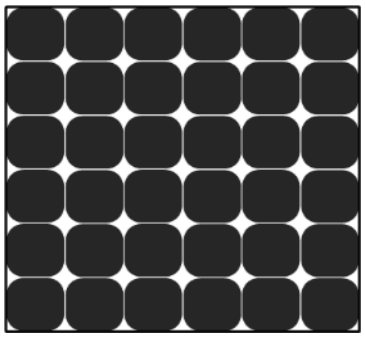

Fig. 1 Monocrystalline Material Based PV Module

To generate enormous power in required range for large PV systems, connecting PV modules in series-parallel is essential. The requisite current level for the system is then obtained by connecting many such strings in parallel [21]. First PV module string is made by joining all the modules in series to get voltage level required. Fig. 2(a) depicts the series-parallel (S-P) configuration. The benefits of series as well as parallel connections can be obtained by connecting the photovoltaic panels in a series-parallel arrangement Partial shading conditions negatively impact the SP

configuration and the overall system's output voltage. In addition, the PV system experiences more considerable mismatch losses [20]. To overcome this drawback a bridge rectifier structure can be used as shown in Fig. (2b).It is called Bridge –link PV array configuration which can minimize the losses in S-P configuration structure, also known as the Bridge-Link (B-L) PV array arrangement, to eliminate the losses in the S-P configuration. By joining two modules in series and then connecting the same modules in parallel, each bridge structure in B-L design can be formed.

The B-L configuration architecture is modified to create the H-C configuration, as shown in Fig. 2(c). The units are joined in this arrangement such that they resemble a honeycomb's hexagonal shape. In this design, the strings have cross-ties in between them. However, H-C configuration is superior to shading patterns of row wise, which is its advantage [21]. The cross-ties in this layout necessitate more cable, which raises cabling cost and causes more losses, which is one of its disadvantages. The other configuration obtained by connecting S-P PV array across each row junction is the T-C-T configuration. [18]. Six modules are linked in parallel when an array is configured as a 6x6. Then, as illustrated in Fig. 2(d), these six strings of parallel-connected modules are joined in series. Individual PV string currents added together make up a T-C-T array's terminal current [22]. The T-C-T design performs better than the others when there is shade, and a considerable GMPP can be generated. However, there is a substantial amount of cross-ties, which means additional wires are required [23].

Fig. 2(e) gives the proposed Triple-Series Parallel-Ladder (T-SP-L) configuration, which has reduced cross ties. The Triple-Series Parallel-Ladder structure can be obtained by joining the cross ties in the S-P PV array for every three stings gap and long cross ties for every three rows. In a 6 x 6 PV array, T-C-T requires 25 cross ties, and T-SP-L requires nine cross ties. 12 cross ties are needed for the H-C as well as B-L PV array configurations. T-S P-L configuration has less cross links than TCT, B-L, H-C configurations. The extraction of maximum power depends upon the amount of crossties and the way of the crossties are connected. In this paper with the help of minimum number of crossties and proper connection of crossties structure the power enhancement has been suggested. In this paper, the cross-tie connection arrangement was chosen to enhance the power with fewer cross-ties. The key benefit of this T-SP-L arrangement is reduction in cross-ties losses as well as an increased power extraction than other configurations.

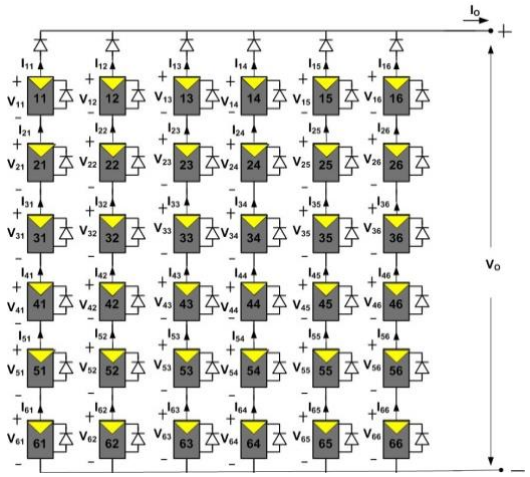

(a)

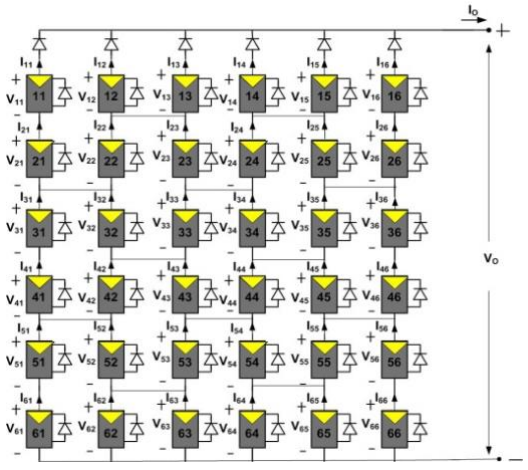

(b)

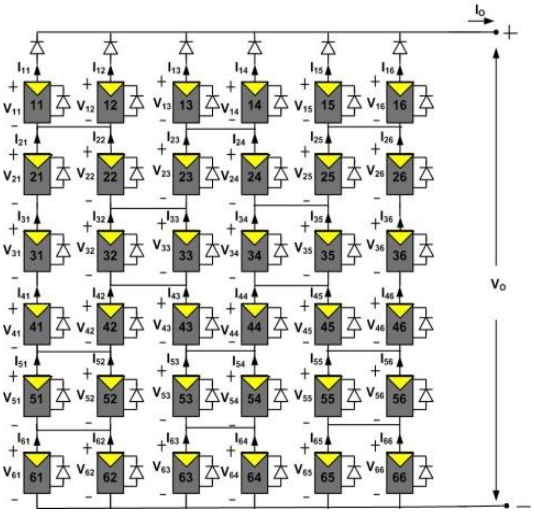

(c)

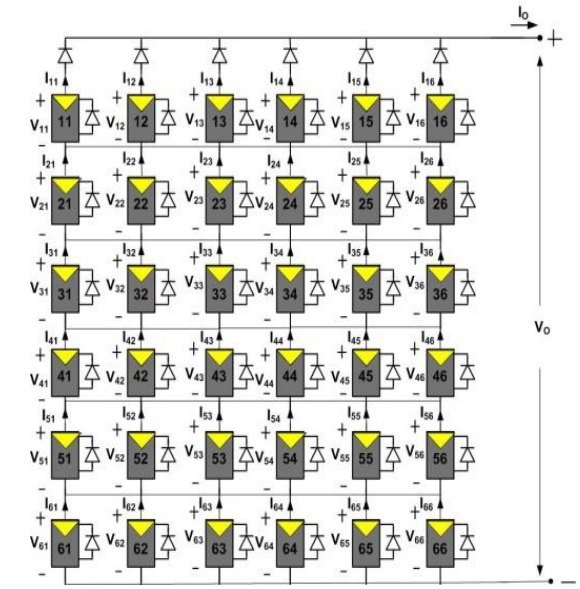

(d)

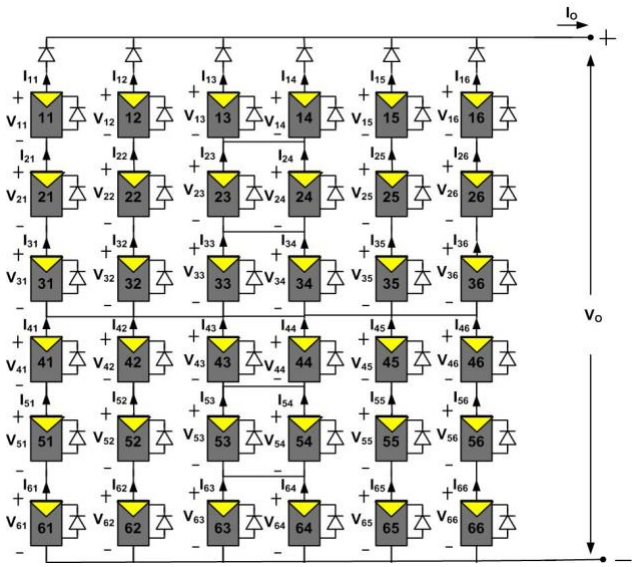

(e)

Fig.2 6X6 PV array topologies (a) Series-Parallel (b) Bridge-Link (c) Honey-comb (d) Total-Cross-Tied (e) Proposed Triple Series Parallel- Ladder

3. Partial Shading Conditions on PV Array Configurations

The impact of partial shading and shading situations considered in this manuscript are discussed in this section. Partially shadowing a PV array has a significant impact on its output power. As partial shadowing may be caused by surrounding structures, buildings, birds' dropouts, etc., improving PV system efficiency is crucial [24]. The shading patterns are categorized according to the intensity of the solar radiation impacting the modules of the array. PV systems exhibit output characteristics which spans multiple MPPs due to shading. PSCs cause PV systems to have mismatch power losses, which lowers the amount of generation as well as capacity and efficiency. Selecting proper material and using appropriate array configurations one of the way to lessen the influence of shading. Five irradiance levels 300 W/m^2, 500 W/m^2, 700 W/m^2, 900 W/m^2 and 1000 W/m^2 are considered as shown in Fig. 3.

Long narrow, short narrow, long wide, short wide, middle shading circumstances are considered for the analysis of considered configurations. The short-wide (SW) shading refers to PSC effects that cause shaded modules to have lengths that are shorter than PV arrays and wider than PV strings [25]. In this case, the modules 11, 21 are under the irradiance of 300 W/m^2, 12, 22, 31,32 are subjected to 500 W/m^2, 13, 23, 33 will receive 700 W/m^2 solar insolation and 1000 W/m^2 irradiance level to the remaining modules. Fig. 3(a) depicts the short wide shading.

If the shading module lengths are short as well as narrow than the width of PV string, it is said to be SN shading condition [26]. For SN condition, the modules 11, 21 are at the irradiance level of 300 W/m^2, 12, 22, 31,32 are subjected to 500 W/m2, 13, 23, 33,41,42,43 will receive 700 W/m^2 solar insolation, 14, 24, 34, 44 are subjected to 900 W/m^2 and 1000 W/m^2 irradiance level to the remaining modules. In Fig. 3(b), the SN shading condition is depicted.

The long wide (LW) shading condition refers to the PSC effects that cause the length of the shaded modules to be longer than the PV string and wider than the PV array's width [27]. For long wide shading condition, the modules 11, 21 are under the irradiance of 300 W/m^2, 12, 22, 31,32 are subjected to 500 W/m^2, 13, 23, 33,41,42,43,51,52,53 will receive 700 W/m^2 solar insolation, 61, 62, 63, are subjected to 900 W/m^2 and 1000 W/m^2 irradiance level to the remaining units. Fig. 3(c) shows the LW shading situation.

The long narrow (LN) shading condition was used because PSC effects will cause shaded modules lengths to be longer than PV strings and narrower than PV array widths [28]. For long wide shading condition, the modules 11, 21 are under the irradiance of 300 W/m^2, 12, 22, 31,32 are subjected to 500 W/m^2, 13, 23, 33,41,42,43,51,52,53 will receive 700 W/m2 solar insolation, 14,15,24,25,34,35,44,45,54,55,61, 62, 63,64,65 are subjected to 900 W/m^2 and 1000 W/m^2 irradiance level to the remaining modules. The shading scenario with LN is given in Fig. 3(d).

The middle (M) shading condition may arise due to the shading of PV array middle part. Fig. 3(e) gives the middle shading situation. For middle shading condition, the modules 22,23,32,33 are exposed to the irradiance of 900 W/m^2, 24, 25, 34,35 are subjected to 700 W/m^2, 42, 43, 52, 53 will receive 300 W/m^2 solar insolation, 44,45,54,55 are subjected to 500 W/m^2 and 1000 W/m^2 irradiance level to the remaining units.

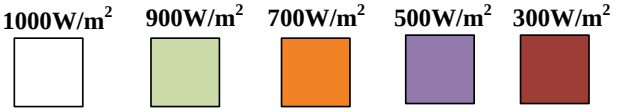

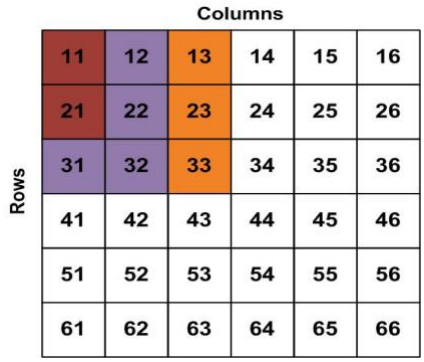

(a)

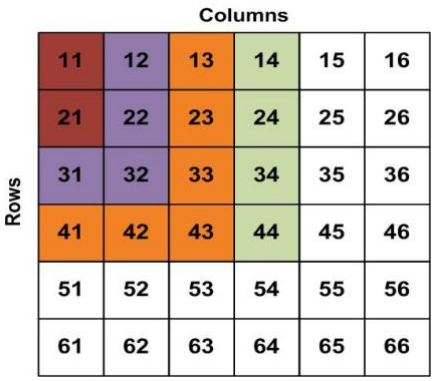

(b)

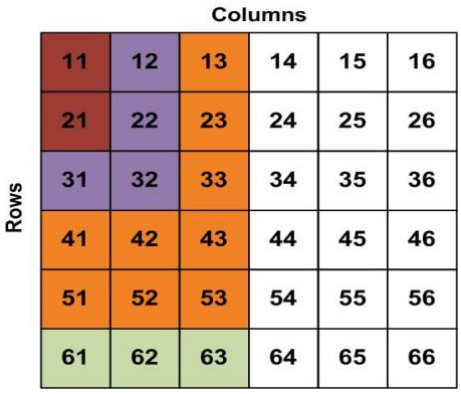

(c)

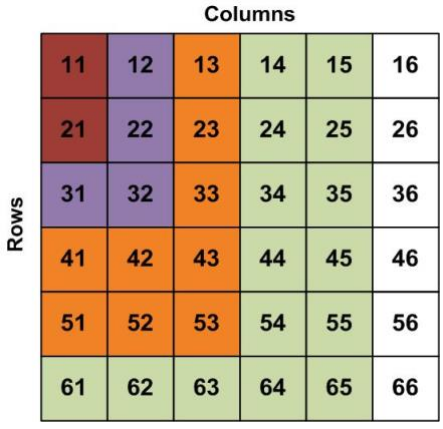

(d)

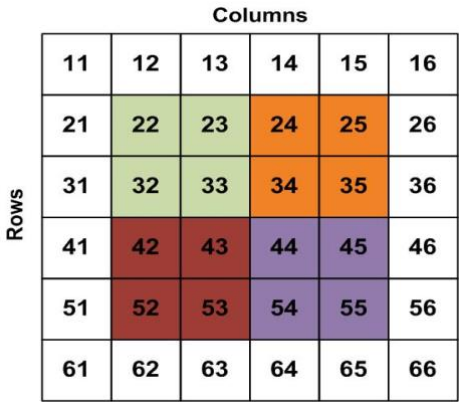

(e)

Fig. 3 (a) Short narrow (b) Short wide (c) Long narrow (d) Long wide (e) Middle shadings

4. PERFORMANCE ANALYSIS AND DISCUSSIONS

Monocrystalline material based PV array of size 6X6 has been considered for performance analysis of proposed and existing configurations under SN, SW, LN, LW, and M shading conditions. The measures used to comment the performance are mismatch losses, global maximum power, and efficiency and fill factor. The monocrystalline PV panel specifications used for simulation have been tabulated in Table 1.

Table 1 Monocrystalline PV panel Specifications

Specifications	Monocrystalline PV Panel
Dimensions of PV panel (mm)	1490x990x42
No of cells in series	54
Module efficiency	14.6%
Short circuit current(A)	8.47
Open circuit voltage(V)	34.63
Maximum current(A)	7.96
Maximum voltage(V)	27.01
Nominal Maximum power(W)	215
Model name	D6M215B5A

4.1 Uniform irradiance shading condition

In uniform shading, all modules are exposed to irradiance level of 1KW/m2. The IV and PV curves of T-SP-L, T-C-T, B-L, S-P and H-C PV array configurations under uniform irradiance are represented in Fig. 4. From Fig.4, it can notice that one global maximum power point exist. Table 2 gives the results of various measures and it can be observed the power same with zero mismatch losses for all conditions with uniform shading.

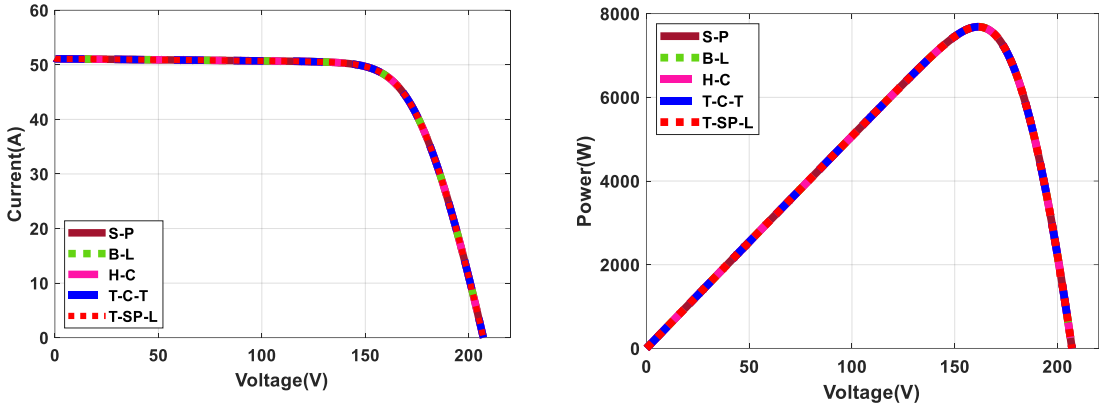

(a) (b)

Fig. 4 (a) Uniform case I-V Curves of (b) Uniform case P-V Curves

Table 2. Results from several measures with uniform irradiance

	V_{oc}	I_{sc}	V_{mp}	I_{mp}	P_{mp}	FF	ML	Efficiency
SP	207.09	51.19	161.38	47.63	7686.15	72.50	0.00	14.47
BL	207.09	51.19	161.38	47.63	7686.15	72.50	0.00	14.47
HC	207.09	51.19	161.38	47.63	7686.15	72.50	0.00	14.47
TCT	207.09	51.19	161.38	47.63	7686.15	72.50	0.00	14.47
TSPL	207.09	51.19	161.38	47.63	7686.15	72.50	0.00	14.47

4.2 Short narrow shading condition

For SN shading situation, the IV & PV curves of T-SP-L, T-C-T, B-L, S-P and H-C PV array configurations are represented in Fig. 5. From Fig. 5, it can observe that three maximum power points are present in PV curves. One point is the global maximum power point in three points, and the other is local. Table 3 shows that the maximum power of 6233.07W produced by T-C-T under short, narrow shading. The next highest power, 6183.96W, produced by the T-SP-L configuration. T-SP-L configuration has generated 216.75W, 191.7W and 280.83W more power than H-C, S-P and B-L configurations. T-SP-L has generated 49.11W less power under SN shading than TCT configuration.

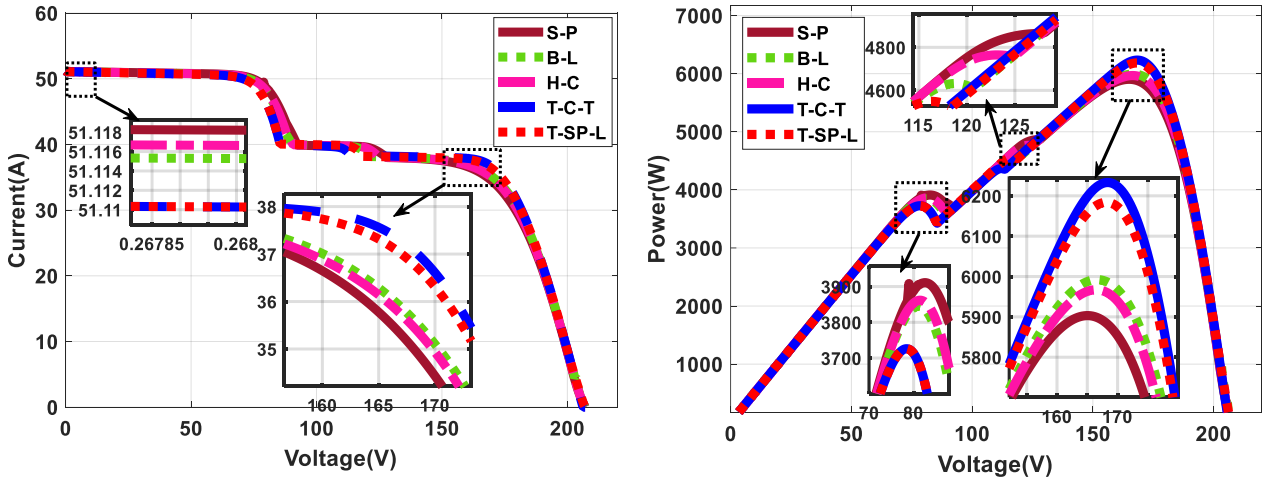

(a) (b)

Fig. 5 (a) SN case I-V Curves (b) SN case P-V Curves

Table 3 Outcomes of several measures with SN condition

	V_{oc}	I_{sc}	V_{mp}	I_{mp}	P_{mp}	FF	ML	Efficiency
SP	207.09	51.19	165.19	35.74	5903.13	55.68	23.20	11.12
BL	207.09	51.19	166.57	35.97	5992.26	56.52	22.04	11.28
HC	207.09	51.19	166.57	35.82	5967.21	56.29	22.36	11.24
TCT	206.39	51.19	168.30	37.04	6233.07	58.99	18.91	11.74
TSPL	207.09	51.19	168.30	36.74	6183.96	58.33	19.54	11.65

4.3 Short wide shading condition

Under SW shading condition, the IV & PV curves of T-SP-L, T-C-T, B-L, S-P and H-C PV array configurations are represented in Fig. 6. From Fig. 6, it can observe that four maximum power points are present in PV curves. In four points, one point is the GMPP, and the remaining are local. Table 4 shows that the highest maximum power of 6068.89W generated by TCT, under short wide shading. The next highest power, 6010.34W, developed by the T-SP-L configuration. T-SP-L configuration generated 177.95W, 143.26W and 212.91W more power than H-C, B-L and S-P. TCT generated 58.55W more power under SW condition than T-SP-L configuration.

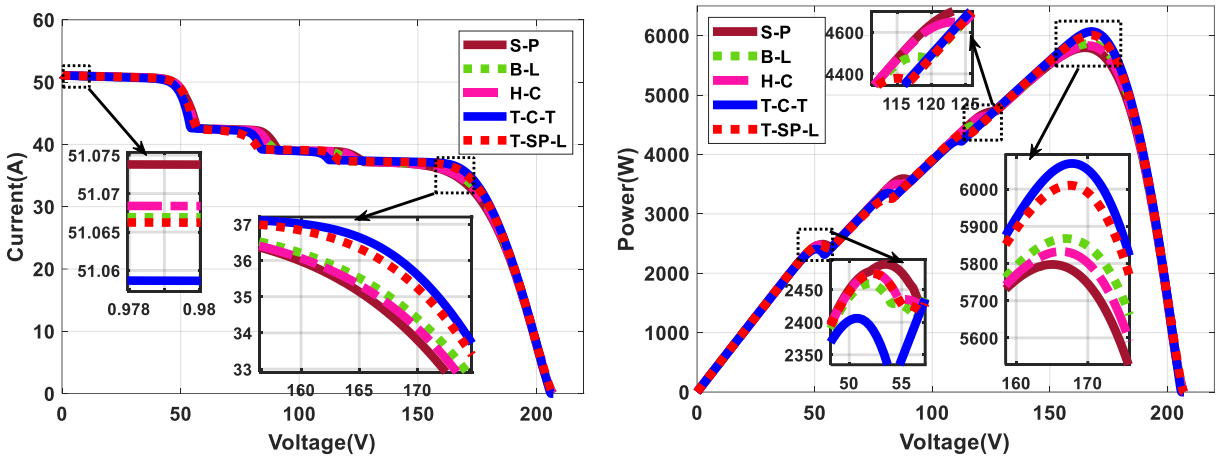

(a) (b)

Fig. 6. (a) SW case I-V Curves (b) SW case P-V Curves

Table 4 Outcomes of several measures with SW condition

	V_{oc}	I_{sc}	V_{mp}	I_{mp}	P_{mp}	FF	ML	Efficiency
SP	207.09	51.19	165.19	35.10	5797.43	54.69	24.57	10.92
BL	206.74	51.19	166.92	35.15	5867.08	55.44	23.67	11.05
HC	206.74	51.19	166.22	35.09	5832.39	55.11	24.12	10.98
TCT	206.05	51.19	167.61	36.21	6068.89	57.54	21.04	11.43
TSPL	207.09	51.19	167.26	35.93	6010.34	56.69	21.80	11.32

4.4 Long narrow shading condition:

For LN shading, the IV & PV curves of T-SP-L, T-C-T, B-L, S-P and H-C PV array configurations under long narrow shading are represented in Fig. 7. From Fig. 7, it can observe that four maximum power points are present in PV curves. Four points are present, one of which is the global maximum power point, and the other three are local. Table 5 shows that highest maximum power of 6130.57Wgenerated by TCT under long narrow shading. The next highest power, 6079.91W, developed by the T-SP-L configuration. T-SP-L configuration generated 145.07W, 117.49W and 211.05W more power than B-L, H-C and S-P. T-SP-L generated 50.66W less power than TCT configuration.

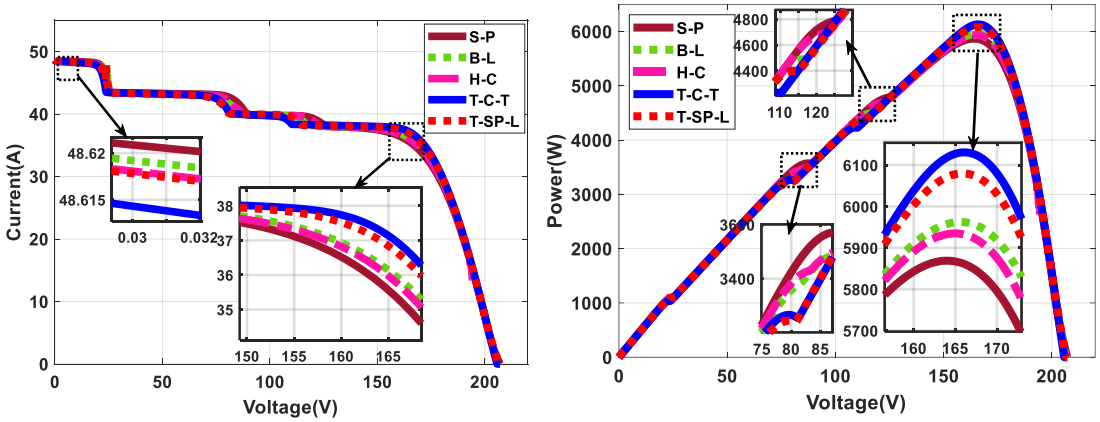

(a) (b)

Fig. 7 (a) LN case I-V Curves (b) LN case P-V Curves

Table 5 Outcomes of several measures with LN condition

	V_{oc}	I_{sc}	V_{mp}	I_{mp}	P_{mp}	FF	ML	Efficiency
SP	207.09	48.63	163.80	35.83	5868.86	58.28	23.64	11.05
BL	206.74	48.63	165.53	36.02	5962.42	59.30	22.43	11.23
HC	206.74	48.63	164.84	36.00	5934.84	59.03	22.79	11.18
TCT	205.70	48.63	165.88	36.96	6130.57	61.29	20.24	11.55
TSPL	206.74	48.63	165.88	36.65	6079.91	60.47	20.90	11.45

4.5 Long wide shading condition

Under LW shading, the IV & PV curves of T-SP-L, T-C-T, B-L, S-P and H-C PV array configurations are represented in Fig. 8. From Fig. 8, it can observe that four maximum power points are present in PV curves. Four points are present, one of which is the GMPP, and the other three are local. Table 6 shows that T-C-T has generated the highest maximum power of 5884.46W under long wide shading. The next highest power, 5835.30W, has been generated by the T-SP-L configuration. T-SP-L configuration has generated 138.5W, 111.38W and 200.74W more power than B-L, H-C and S-P. Compared to the T-C-T PV array arrangement, T-SP-L has generated 49.16W less power.

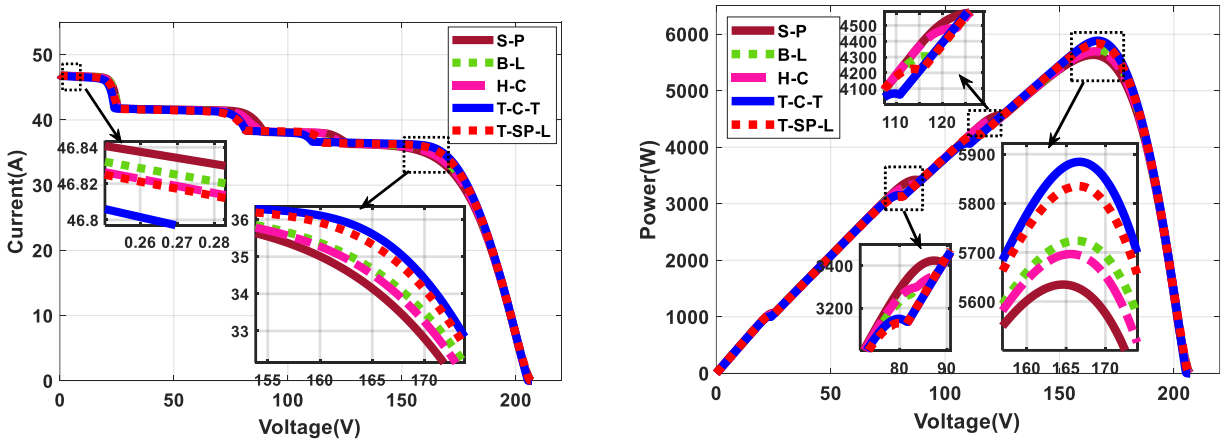

(a) (b)

Fig. 8 (a) LW case I-V Curves (b) LW case P-V Curves

Table 6 Outcomes of several measures with LW condition

	Voc	I_{sc}	V_{mp}	I_{mp}	P_{mp}	FF	ML	Efficiency
SP	207.09	46.92	164.49	34.25	5634.56	57.98	26.69	10.61
BL	206.39	46.92	166.22	34.43	5723.92	59.10	25.53	10.78
HC	206.39	46.92	165.53	34.42	5696.80	58.82	25.88	10.73
TCT	205.70	46.92	166.57	35.33	5884.46	60.97	23.44	11.08
TSPL	206.39	46.92	166.57	35.03	5835.30	60.25	24.08	10.99

4.6 Middle shading condition

Under middle shading condition, IV & PV curves of T-SP-L, T-C-T, B-L, S-P and H-C PV array configurations are represented in Fig. 9. From Fig. 9, it can observe that three maximum power points are present in PV curves. The global maximum power point is one of the three points, and the other two are the local maximum power points. Table 7 shows that T-C-T produced the highest maximum power of 5177.27 under middle shading. The next highest power, 5065.37W, has been generated by T-SP-L configuration. T-SP-L configuration has generated 117.58W, 113.97W and 274.2W more power than H-C, B-L and S-P. The T-C-T PV array layout provided 111.9W more power than T-SP-L, on the other hand.

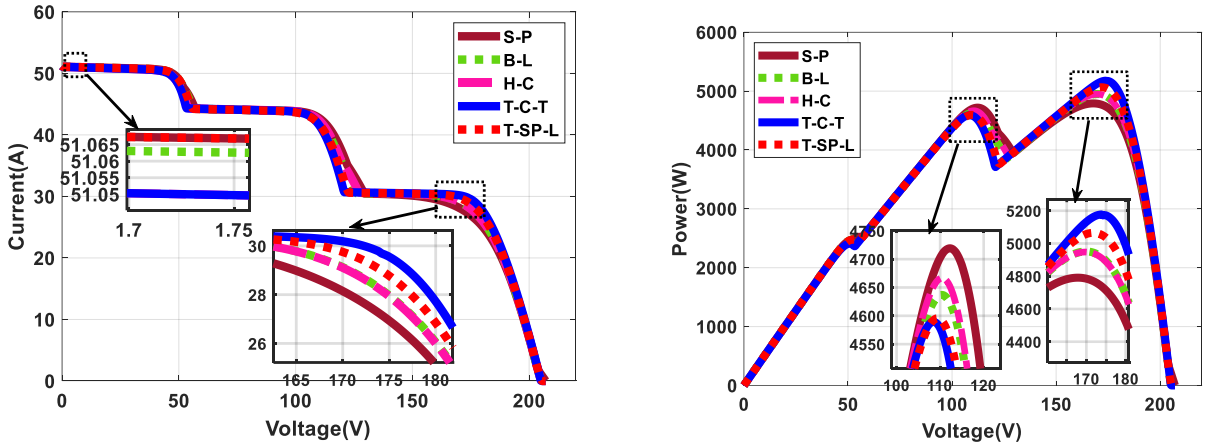

(a) (b)

Fig. 9 (a) Middle case I-V Curves (b) Middle case P-V Curves

Table 7 Outcomes of several measures with Middle condition

	V_{oc}	I_{sc}	V_{mp}	I_{mp}	P_{mp}	FF	ML	Efficiency
SP	207.09	51.19	167.61	28.59	4791.17	45.19	37.66	9.02
BL	205.36	51.19	169.69	29.18	4951.40	47.10	35.58	9.32
HC	205.36	51.19	169.69	29.16	4947.79	47.07	35.63	9.32
TCT	205.36	51.19	173.84	29.78	5177.27	49.25	32.64	9.75
TSPL	205.70	51.19	171.76	29.49	5065.37	48.10	34.10	9.54

5. CONCLUSION

This paper proposes a monocrystalline PV material-based Triple-Series Parallel-Ladder (T-SP-L) PV array topology. The performance of proposed configuration has been examined by 6X6 PV array and compared with S-P, T-C-T, B-L and H-C configurations. The proposed topology has few cross ties than S-P, T-C-T B-L, and H-C configurations. All these configurations performance under uniform, long narrow, short narrow, long wide, short wide and middle shadings has been analyzed. The performance of all

configurations has been measured with various factors. It can be noticed from the results that:

- Under uniform shading, the maximum power is the same and zero mismatch losses for all the configurations.
- In the 6X6 PV array, 16 cross ties have been reduced with the help of T-SP-L connection than T-C-T connection and 3 cross ties reduced than H-C, B-L connections, respectively.
- Under SW, SN, LW, LN, and M shadings, T-SP-L has generated more power than H-C, S-P and B-L configurations with the minimum amount of cross ties compared to T-C-T, B-L and H-C configurations.
- Under SN shading, the proposed topology yields improvement in maximum power compared to S-P is 4.7%, B-L is 3.19% and H-C is 3.63%.
- Under SW shading, the proposed topology yields improvement in maximum power compared to S-P is 3.67%, B-L is 2.38% and H-C is 2.96%.
- Under LN shading, the proposed topology yields improvement in maximum power compared with S-P is 3.59%, B-L is 1.97% and H-C is 2.44%.
- Under LW shading, the proposed topology yields improvement in maximum power compared with S-P is 3.56%, B-L is 1.94% and H-C is 2.43%.
- Under M shading, the proposed topology yields improvement in maximum power compared with S-P is 5.72%, B-L and H-C is 2.3%.

References

[1] Q. Chen and Y. Wang, "Research Status and Development Trend of Concentrating Solar Power", 9th International Conference on Renewable Energy Research and Application (ICRERA), Glasgow, UK, 2020, pp. 390-393.

[2] P.C. Choubey, A. Oudhia and R. Dewangan, "A Review: Solar Cell Current Scenario and Future Trends", Recent Research in Science and Technology, Vol.4, No.8, 2012, pp. 99-101.

[3] A. McEvoy, L. Castaner and T. Markvart, "Solar Cells: Materials, Manufacture and Operation", 2nd Edition, Elsevier Ltd., Oxford, 3-25.

[4] V.V. Tyagi, Nurul A.A. Rahim, N.A. Rahim and J.Selvaraj, "A Progress in solar PV technology: Research and achievement", Renewable and Sustainable Energy Reviews, 2013, Vol. 20, pp.443–461.

[5] C. Becker, T. Sontheimer, S. Steffens, S. Scherf, and B. Rech, "Polycrystalline silicon thin films by high rate electron beam evaporation for photovoltaic applications-Influence of substrate texture and temperature" Energy Procedia, Vol.10, 2011, pp.61-65.

[6] K. Yamamoto, A. Nakajima, M. Yoshimi, T. Sawada, S. Fukuda, T. Suezaki, M. Ichikawa, Y. Koi, M. Goto, T. Meguro, T. Matsuda, M. Kondo, T. Sasaki, Y. Tawada, "A high efficiency thin film silicon solar cell and module", Solar Energy, Vol. 77, No. 6, 2004, pp. 939-949.

[7] H.I. Dag, M.S. Buker, "Performance evaluation and degradation assessment of crystalline silicon based photovoltaic rooftop technologies under outdoor conditions", Renewable Energy, vol. 156, 2020, pp. 1292-1300.

[8] C. B. Isabela, R.A.M. Lameirinhas, J. N. Torres, and A.F. Carlos, "Comparative study of the copper indium gallium selenide (CIGS) solar cell with other solar technologies", Sustainable Energy & Fuels, Vol. 5, No. 8, 2021, pp. 2273-2283.

[9] V. Sarayu, M.VanithaSri and A.RamaKoteswaraRao. "Performance analysis of mono crystalline, poly crystalline and thin film material based 6 × 6 T-C-T PV array under different partial shading situations", Optik, vol. 248, 168055, 2021, pp. 1-14.

[10] A.D. Dhass, R.S. Kumar, P.Lakshmi, E.Natarajan, A.Arivarasan, "An investigation on performance analysis of different PV materials", Materials Today: Proceedings, Vol. 22, No.3, 2020, pp. 330-334.

[11] R.Deep, A. Agarwal, A. Mishra, "A study and comparative analysis of various materials based solar photovoltaic module to improve the output performance", Materials Today: Proceedings, Vol. 22, No.4, 2020, pp.3203-3212.

[12] S. R. Pendem and S. Mikkili, "Modelling and performance assessment of PV array topologies under partial shading conditions to mitigate the mismatch power losses", Solar Energy, Vol.160, 2018, pp.303-321.

[13] P. K. Bonthagorla and S. Mikkili "A Novel Fixed PV Array Configuration for Harvesting Maximum Power from Shaded Modules by Reducing the Number of Cross-Ties", IEEE Journal of Emerging and Selected Topics in Power Electronics, Vol.9, No.2, 20020, pp.2109-2121.

[14] F. Ghasemzadeh, M. Esmaeilzadeh, M. E. Shayan, "Photovoltaic Temperature Challenges and Bismuthene Monolayer Properties" Int. J. Smart Grid (ijSmartGrid), Vol.4 no.4, 2020, pp.190-195.

[15] M.K. Sharma, and J.Bhattacharya, "Dependence of spectral factor on angle of incidence for monocrystalline silicon based photovoltaic solar panel", Renewable Energy, Vol.184, 2022, pp.820-829.

[16] T.Hidayat, E. Nurcahyo and W.P.Muljanto, "Comparative Analysis of the Performance of

Monocrystalline, Polycrystalline, and Monocrystalline Solar Cells Coated with Graphene", International Journal of Scientific Engineering and Science, Vol.6, No.2, 2022, pp.78-82.

[17] M.Tawalbeh, A. Al-Othman, F.Kafiah, E.Abdelsalam, F.Almomani and M. Alkasrawi, "Environmental impacts of solar photovoltaic systems: A critical review of recent progress and future outlook", Science of The Total Environment, Vol.759, 2021, pp.143528.

[18] K.Rajani, and T.Ramesh, "Reconfiguration of PV arrays (TCT, BL, HC) by considering wiring resistance", CSEE Journal of Power and Energy Systems, Vol.8, No.5, 2022, pp.1408-1416.

[19] F. Javed, "Impact of Temperature & Illumination for Improvement in Photovoltaic System Efficiency", Int. J. SMART GRID (ijSmartGrid), Vol.6, no.1, 2022, pp.13-22.

[20] K.Rajani and T.Ramesh, "Impact of Wiring Resistance on PV Array Configurations in Harvesting the Maximum Power Under Static and Dynamic Shading Conditions", IETE Journal of Research, 2022, pp.1-29.

[21] S.R.Pendem, and S.Mikkili, "Modeling, simulation, and performance analysis of PV array configurations (Series, Series-Parallel, Bridge-Linked, and Honey-Comb) to harvest maximum power under various Partial Shading Conditions", International journal of green energy, Vol.15, No.13, 2018, pp. 795-812.

[22] V.B.Raju, and C.Chengaiah, "Enhance the Output Power of a Shaded Solar Photovoltaic Arrays with Shade Dispersion based TCT Configuration", Trends in Renewable Energy, Vol.7, No.1, 2021, pp.1-23.

[23] K.Rajani, and T.Ramesh, "An Automatic Column Wiring Resistance Algorithm for Static Reconfiguration of PV Arrays and Analysis of Reconfigured T-C-T and T-T-C-L under Dynamic Shading Conditions", J Control Autom Electr Syst., 2023.

[24] W. A. Abri, R. A. Abri, H. Yousef and A. Al-Hinai, "A Global MPPT Based on Bald Eagle Search Technique for PV System Operating under Partial Shading Conditions", 10th International Conference on Smart Grid (icSmartGrid), Istanbul, Turkey, 2022, pp. 325-332.

[25] N.D.Kumar, T.A.R. Kumar and A.R.K. Rao, "Effect of Partial Shading on the Performance of Various 4× 4 PV Array Configurations", ECTI Transactions on Electrical Engineering, Electronics, and Communications, Vol.20, No.3, 2022, pp.427-437.

[26] R.K.Pachauri, J.Bai, I.Kansal, O.P.Mahela, and B. Khan, "Shade dispersion methodologies for performance improvement of classical total cross-tied photovoltaic array configuration under partial shading conditions", IET Renewable Power Generation, Vol.15, No.8, 2021, pp.1796-1811.

[27] B.Yang, H.Ye, J.Wang, J.Li, S.Wu, Y. Li, H. Shu, Y. Ren and H.Ye, "PV arrays reconfiguration for partial shading mitigation: Recent advances, challenges and perspectives", Energy Conversion and Management, Vol.247, 2021, pp.114738.

[28] G.Yu, H.Yang, D.Luo, X.Cheng, and M.K.Ansah, "A review on developments and researches of building integrated photovoltaic (BIPV) windows and shading blinds", Renewable and Sustainable Energy Reviews, Vol.149, 2021, pp.111355.

[29] A. Belkaid, I. Colak, K. Kayisli and R. Bayindir, "Improving PV System Performance using High Efficiency Fuzzy Logic Control," 8th International Conference on Smart Grid (icSmartGrid), Paris, France, 2020, pp. 152-156.

[30] P.V.Mahesh, S. Meyyappan, and A.R.K.Rao, "Maximum power point tracking using decision-tree machine-learning algorithm for photovoltaic systems. Clean Energy, Vol.6, No.5, 2022, pp.762–775.

[31] P.V.Mahesh, S. Meyyappan, and A.R.K.Rao, "Support Vector Regression Machine Learning based Maximum Power Point Tracking for Solar Photovoltaic Systems", International Journal of Electrical and Computer Engineering Systems, Vol.14,No.1, 2023, pp.100-108.

[32] D. Yousri, E. F. El-Saadany, Y.Shaker, T. Sudhakar Babu, A.F. Zobaa, D. Allam, "Mitigation of power loss from mismatching series-parallel and total-crossed array configurations using a new hunger-game search optimizer enhanced heterogeneous'", Energy Reports Vol.8, 2022, pp.9805–9827.

[33] M.Jayachandran, Ch. Rami Reddy, P.Sanjeevikumar, and A. H. Milyani, "Operational planning steps in smart electric power delivery system", Scientific Reports, Vol.11, No.1, 2021, pp.17250.

[34] B.V.Rajanna, "Grid Connected Solar PV System with MPPT and Battery Energy Storage System", International Transactions on Electrical Engineering and Computer Science, Vol.1, No.1, 2022, pp.8-25.